J. Microbiol. Biotechnol. (2012), **22**(1), 34–45
http://dx.doi.org/10.4014/jmb.1105.05055
First published online November 3, 2011

JOURNAL OF MICROBIOLOGY AND BIOTECHNOLOGY

Effect of Ion Pair on Thermostability of F1 Protease: Integration of Computational and Experimental Approaches

Rahman, Raja Noor Zaliha Raja Abd[1]*, Noor Dina Muhd Noor[1], Noor Azlina Ibrahim[1], Abu Bakar Salleh[1], and Mahiran Basri[2]

Enzyme and Microbial Technology Research Group, [1]Faculty of Biotechnology and Biomolecular Sciences, [2]Faculty of Science, University Putra Malaysia, 43400 UPM Serdang, Selangor, Malaysia

Received: May 27, 2011 / Revised: August 12, 2011 / Accepted: September 15, 2011

A thermophilic *Bacillus stearothermophilus* F1 produces an extremely thermostable serine protease. The F1 protease sequence was used to predict its three-dimensional (3D) structure to provide better insights into the relationship between the protein structure and biological function and to identify opportunities for protein engineering. The final model was evaluated to ensure its accuracy using three independent methods: Procheck, Verify3D, and Errat. The predicted 3D structure of F1 protease was compared with the crystal structure of serine proteases from mesophilic bacteria and archaea, and led to the identification of features that were related to protein stabilization. Higher thermostability correlated with an increased number of residues that were involved in ion pairs or networks of ion pairs. Therefore, the mutants W200R and D58S were designed using site-directed mutagenesis to investigate F1 protease stability. The effects of addition and disruption of ion pair networks on the activity and various stabilities of mutant F1 proteases were compared with those of the wild-type F1 protease.

Keywords: Site-directed mutagenesis, thermostability, ion pairs

To date, the stability of subtilisin has been most amenable to enhancement. However, it is poorly understood [4]. Most subtilisin engineering has involved catalytic amino acids, substrate binding, and stabilizing mutations to meet the requirements that are needed for industrial applications. A major requirement for commercial processes that use enzymes is the thermal stability of the enzyme because thermal denaturation is a common cause of enzyme inactivation. Furthermore, thermostable enzymes are needed in industrial settings as a result of their ability to withstand harsh operating conditions [10].

To gain insight into the thermostability of proteins, structurally homologous proteins with different thermostabilities have been compared using known crystal structures or predicted structures from homology modeling [5, 39]. Kumar *et al*. [17] have analyzed the sequence and structural factors that enhance protein thermostability in 18 nonredundant families of homologous thermophilic and mesophilic proteins. These factors include amino acid composition, proline substitution in loops, α-helical content, α-helix geometry, polar/nonpolar surface area that is buried or exposed in water, insertion/deletions, hydrogen bonds, and salt bridges. Other modifications of disulfide bonds [28, 35], hydrophobic interactions [34], calcium binding [3, 12], and free energy [29] have been used to study the stability of proteins. A common trend that is apparent from analysis of the structures that have been identified so far in hyperthermophiles suggests that an increased number of ion pair networks contribute to the observed extreme thermostability [15, 39]. Higher thermostability in stetterlysin and pyrolysin with the subtilases from mesophilic and thermophilic origin, that is subtilisin BPN' and thermitase, correlates with an increased number of residues that are involved in ion pair networks and aromatic interactions [39].

Experimentally, the thermophilic *Bacillus* strain F1 has a half-life of 4 h at 85°C, and 25 min at 90°C, and is stable between pH 7.0 and pH 10 for 24 h at 70°C without any loss of activity [9, 30]. In this report, the F1 protease sequence and structure were compared with its mesophilic (subtilisin BPN') and hyperthermophilic (pyrolysin and stetterlysin) homologs. A modeled structure was used to predict the protein engineering of residues that were crucial to the stability of thermophilic *B. stearothermophilus* F1 protease. In the meantime, two types of mutations [W200R, in which tryptophan (Trp) at position 200 was replaced by arginine

*Corresponding author
Phone: +603-89467592; Fax: +603-89467593;
E-mail: rnzaliha@biotech.upm.edu.my

(Arg); D58S, in which aspartic acid (Asp) at position 58 was replaced by serine (Ser)] were designed to generate additional potential ion pairs or to disrupt the existing ion pairs in F1 protease, respectively. The effects of these substitutions on the stability of F1 protease were monitored using modeling, thermostability tests, and circular dichroism (CD) structure analyses.

MATERIALS AND METHODS

Model Building

The F1 protease gene was sequenced and deposited at the GenBank database at NCBI with the accession number of AY028615. The F1 sequence was aligned with templates Ak1 protease (1DBI) and thermitase (1THM) using the Homology module of InsightII (MSI, CA, USA). Both enzymes have been successfully crystallized. This target-template alignment was logged onto a server running Modeller Version 4 [32]. Refinement of the best initial model was done using the Auto-Rotamer and by manually rotating the side chains (Homology module). The minor steric clashes and bond strain due to the building of the model were regularized using Discover (MSI, CA, USA) and the corresponding Consistent Valence Force Field (CVFF) parameter (Biosym/MSI). Hydrogen atoms were added to the model structure according to the standard geometries. The final model was evaluated to ensure its accuracy by using three independent methods from the Internet: Procheck [17], Verify3D [19], and Errat [6]. Backbone conformation was evaluated by Procheck. The Verify3D was for determining protein 3D structure, and developing and verifying the correctness of a final protein structure. Errat works by analyzing the statistics of nonbonded interactions between atom types. The structural similarity between the model and the template from the PDB was assessed from the RMSD value.

Factor Enhancing Protein Thermostability

The final model of F1 protease was analyzed and compared with subtilisin BPN' (mesophilic), and stetterlysin and pyrolysin (hyperthermophilic) in terms of possible ion pairs formation, amino acid compositions, disulfide bonds, and aromatic interaction. Analyses were performed using ptraj, a program feature by AMBER.

Molecular Dynamics Simulations

Molecular dynamics (MD) simulations and energy minimizations were carried out on a PC using the AMBER 6 suite program. MD simulations were carried out in periodic boundary condition (water molecules) at 360 K, equivalent to 85°C, the optimum temperature for wild-type F1 protease activity [29]. Mutated structures were performed with InsightII (Accelrys Inc., CA, USA) implemented on Silicon Graphics O2. Analyses were performed using ptraj, a program feature by AMBER, which allows processing of coordinates and trajectories. Analyses based on RMSD, β-factor, and ion pair interactions were performed.

Construction of Mutated F1 Protease

In this method, the pTrcHis/F1 protease gene (wild type) from *E. coli* XL1 Blue was used for producing the mutants W200R and D58S. Both of these substitutions were introduced in a single mutant. The replacements of Trp at amino acid 200 by Arg (W200R), and Asp at position 58 by Ser (D58S) were performed by using the GeneTailor Site Directed Mutagenesis System. In the methylation reaction step, the recombinant F1 protease gene (pTrcHis/F1) was mixed with other reagents; 1.6 μl of methylation buffer, 1.6 μl of 10× SAM, 1.0 μl of DNA methylase, and 16 μl of sterile distilled water. The reagent mixture was incubated at 37°C for 1 h. In this reaction, the methylated plasmid for each was amplified with two overlapping primers. The primers designed for W200R were 5'-cattctcgaactatggaacaagggtagatgtcgt-3', 5'-tgttccatagttcgagaatgatgctaaccg-3'; and for D58S were 5'-gaaaagtcatcaaaggatat **tc**tttcgtagataa-3', 5'-atatcctttgatgacttttccatctaaatct-3' [bold letter(s) is the forward primer contains the target mutation]. The reaction was amplified in a thermocycler (GeneAmp PCR System 2400, Perkin Elmer). To detect PCR product, the PCR mixture was electrophoresed through an agarose gel (1%) at 80 mA for 0.5 h, and then the gel was stained with ethidium bromide (1 μg/ml) for 10 min. After confirmation of the single mutation on the F1 protease gene, the mutated genes were cloned into the pGEX-4T1 vector using two primers, pGEX-pro (5'agca*gaattc*gcctctaatgatggg3') and pGEX-rev (5'aatctat*ctcgag*ttaatat gttacagc 3'). An *Eco*RI site and a *Xho*I site were introduced for each of the primers respectively. Using pGEX-pro, the mutated protease gene only amplified the prosequence and mature sequence of the mutated F1 protease gene with the size of ~1.2 kb. The temperature profile for pGEX-pro and pGEX-rev to run the PCR was 94°C/ 3 min for one cycle, (94°C/ 1 min, 55°C/ 1 min, 72°C/ 1 min) × 25 cycles, and 72°C/7 min for one cycle.

Transformation the Mutated PCR Product

The products of pTrcHis/wild-type and two mutant genes (W200R and D58S) were transformed into MrcBC *E. coli* DH5α-T1. The mixture was incubated on ice for 7–10 min, and then incubated for 30 s in a 42°C water bath without shaking and then immediately transferred to ice for 1 min. Two hundred μl of SOC medium that was kept at room temperature was added to the tube. The tube was capped tightly and shaken horizontally (150 rpm) at 37°C for 1 h. The mixture (50 μl) was spread on LB plates containing ampicillin (50 μg/ml) and incubated at 37°C overnight. The mutated genes constructed into the pGEX-4T1 vector were transformed into *E. coli* BL21(DE3)pLysS. This transformation medium was plated onto Luria Bertani–Skim Milk Agar (LB–SMA containing 2% of skim milk agar) plates containing ampicillin (50 μg/ml) and chloramphenicol (35 μg/ml), and incubated at 37°C overnight.

Identification of the Mutated Gene Fragment

Single colony PCR was done by using a PCR cocktail reaction, consisting of PCR buffer, dNTP, primers, and *Taq* polymerase. The pTrcHis and pGEX forward sequence primer and PCR product reverse primer were used in this reaction. Recombinant plasmids containing the mutated gene fragment were identified by restriction enzyme analysis using *Nco*I and *Eco*RI (vector pTrcHis) and *Eco*RI and *Xho*I (vector pGEX-4T1). Both PCR product and digested plasmid were checked by running on 1% agarose gel electrophoresis at 80 mA and the gel was stained with ethidium bromide (1 μg/ml) for 10 min. Ten colonies were also picked and streaked on the LB–SMA plates as well as LB agar plates. The LB–SMA plates were incubated at 37°C overnight, and transferred to 60°C for 5 to 10 h to see the haloes produced by the protease. The nucleotide sequence

was determined by sending recombinant plasmids for automated sequencing. Samples were sequenced using an ABI PRISM 377 Genetic Analyzer (Perkin-Elmer). Analyses of the sequences were done by using BLAST from the National Center of Biotechnology (NCBI) (http://www.ncbi.nih.gov), Expasy Molecular Biology server (http://expasy.org/tools).

Expression of Recombinant F1 Protease and its Mutant in *E. coli* BL21(DE3)pLysS/pGEX and Their Purification

E. coli BL21(DE3)pLysS harboring recombinant plasmids was grown for 3 h in a 500 ml Schott Duran bottle containing 100 ml of LB medium supplemented with ampicillin (50 μg/ml) and chloramphenicol (35 μg/ml) in a rotary shaker (150 rpm) at 37°C. The cultures were induced with 0.1 mM IPTG at OD_{660nm} ~ 0.5 for 24 h. The cultures were harvested by centrifugation and resuspended with 0.1 M Tris-HCl–2 mM $CaCl_2$ buffer before sonication (Branson Sonifier 250: duty cycle 30, output 2, and 2 min) and cleared by centrifugation (8,000 ×*g*, 30 min). The clear crude lysate was assayed to detect protease production. For purification, the culture supernatants were prepared by removing the cells in the culture by centrifuging 1,000 ml of the culture at 8,000 ×*g* for 30 min. The precipitated cells were resuspended in 100 ml of PBS buffer (pH 7.4) and disrupted by sonication using an ultrasonic disruptor (Branson Sonifier 250: duty cycle 30, output 2, and 2 min) in an ice bath. Cell extract was obtained by centrifugation at 8,000 ×*g* at 4°C for 30 min. The recombinant F1 protease and its mutant contained in these crude cell extracts were purified by affinity chromatography with a glutathione Sepharose (GE Healthcare, Germany) column (2×5 cm) equilibrated with PBS buffer (pH 7.4) at 4°C. The binding protein was eluted at 1 ml/min with glutathione reduced-Tris-HCl buffer (pH 8.0). Fractions of 3 ml were collected and measured for absorbance at 280 nm and protease activity. The collected fraction with high activity was purified by heat treatment at 70°C for 1 h. The heat-treated enzyme was then centrifuged at 8,000 ×*g* for 15 min to remove denatured protein. Purified enzymes of recombinant F1 protease, W200R mutant, and D58S mutant genes were used for further optimization and characterization studies.

Measurement of Proteolytic Activity

Protease activity was determined by the azocasein hydrolysis method, which was slightly modified from Rahman *et al*. [30]. Azocasein, 0.5% (w/v) (Sigma, USA) dissolved in 0.1 M Tris-HCl–2 mM $CaCl_2$, pH 9.0, was pipetted into vials and preincubated at 70°C. The reaction was initiated by addition of 0.1 ml of an enzyme solution and was incubated at 70°C for 30 min. The reaction was stopped by the addition of 1.1 ml of a trichloroacetic acid (TCA) 10% (w/v). The TCA was added to precipitate the unhydrolyzed protein. The mixture was allowed to stand at room temperature for 30 min before centrifugation in an eppendorf tube at 13,000 ×*g* for 10 min. The supernatant fluid was removed from each tube and mixed with an equal volume of NaOH (1 N). The absorbance was read at 450 nm using a spectrophotometer (Pharmacia). Control samples were assayed in the same manner as the test samples, except the enzyme was added at the end of the incubation period after the addition of TCA. All enzyme assays were carried out in triplicate. One unit of azocasein activity was defined as the enzyme at equivalent to an absorbance changed of 0.001 per minute at 70°C under the standard assay condition. Activities were also measured according to the formula: $U = \Delta A_{450} \times 1{,}000\ min^{-1}$.

Characterization of Recombinant F1 Protease and Mutants

Thermostability of the recombinant F1 protease, and W200R and D58S mutants was checked in the presence of 2 mM Ca^{2+} for different durations at two different temperatures, 85°C and 90°C. Secondary structure analysis and thermal denaturation (melting point, T_m) studies for the wild type and its mutants were determined by using the Far-UV CD spectrum J-810 (Jasco, Japan). For secondary structure analysis, the near-UV (190–250 nm) spectra was obtained using a solution containing protein (0.1 mg/ml) in 10 mM sodium phosphate buffer (pH 8.0) and were analyzed at 20°C using a 0.1 cm optical path cell. Each of sample proteins were repetitively scanned at least three times for each of triplicate data sets, and the average value was used for the analysis. The data were converted to mean residue ellipticity (measured in deg cm^2/dmol). The compositions of secondary structure were calculated by using the program supplied with the instrument. Finally, variable temperature measurements of proteins were performed for thermal denaturation studies, which employed a 2 mm cell at 221 nm. The warm-up period was 50°C to 90°C with the temperature raised by 1°C increment. The transition curve for thermal denaturation was analyzed using a two-state transition model and the linear extrapolation method.

Results and Discussion

Model Building and Evaluation of the Predicted F1 Protease Structure

For closely related protein sequences with identities that are higher than 30–40%, the alignments that are produced by all methods are correct [37]. The F1 protease gene has sequence similarities with other serine protease genes: Ak1 protease at 96% [33] and thermitase at 61% [36] (Fig. 1). From the four generated models (models A, B, C, and D) that were constructed using Modeller, the quality of the Ramachandran plots and Errat analyses revealed that model C (which was generated from thermitase as a template) was better than the other models (Table 1). Therefore, model C was selected as the best model for further refinement and evaluation.

Table 1. Quality of structures predicted by the Modeller program.

Rough model	Ramachandran plot quality (%)			Errat (%)[b]
	Allowed[a]	General	Disallowed	
Model A[c]	98.4	0.8	0.8	89.3
Model B[c]	96.2	2.1	1.7	90.8
Model C[d]	98.8	0.8	0.4	95.2
Model D[d]	98.8	0.8	0.4	86.8
Model E[e]	100.0	-	-	96.3

[a]Ramachandran plot qualities show the amount (%) of residues belonging to most favored allowed and additional allowed regions.
[b]Errat qualities show the amount (%) of residues below the 95% confidence limit.
[c]The rough model generated from Ak1 protease as template.
[d]The rough model generated from thermitase as template.
[e]The refined model from rough Model C.

Fig. 1. Structure-based alignment of the amino acid sequences of pyrolysin (Pyr), stetterlysin (STT), F1 protease (F1P), Ak1 protease (Ak1), thermitase (THM), and subtilisin BPN' (BPN).

Catalytic residues D39*, H72*, and S226* are indicated by (*). Grey shading indicates residues of Pyr, STT, and BPN that are the same as F1P. Residues that are identical between F1P, Ak1, and THM are highlighted with darker shading. The boxed amino acid residues represent residues involved in ion pair networks that were used to design the mutant protease; D58S and W200R protease.

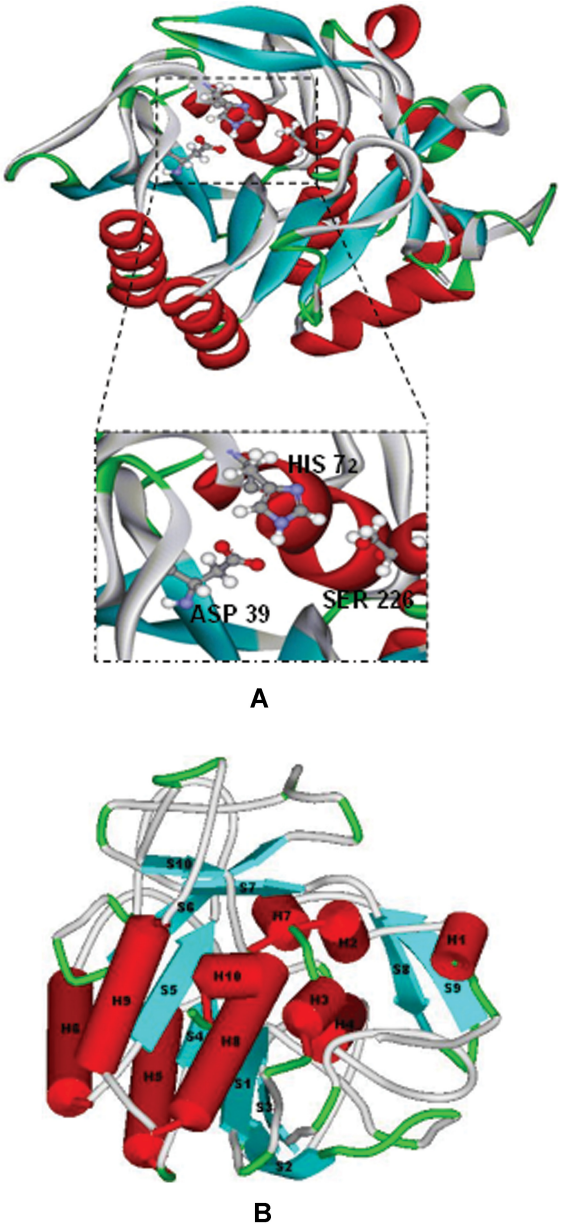

Fig. 2. The predicted structure for F1 protease.
(**A**) The predicted structure shown with the secondary structure rendered as a ribbon. F1 protease contains a catalytic triad, comprising Asp 39, His 72, and Ser 226 (ball-and-stick), similar with other serine proteases. (**B**) Schematic representation of the secondary structure topology of F1 protease. The F1 protease structure comprises 10 α-helices (red), 10 β-sheets (blue-green, bluish), turn (green), and coil (grey), arranged in a single domain.

Using PROCHECK, the Ramachandran plot for the F1 structure represented approximately 87% of the residues in most of the favored regions. No residue was detected in generously allowed regions. Comparing this result with that of thermitase (1THM), we found nine residues that were located in general allowed regions. Therefore, the results suggest that the backbone conformations of the final model of F1 protease are better than those of the template. The second evaluation was performed using VERIFY3D or 3D-1D profiles. The correctness of the predicted F1 structure was detected based on the average score of +0.42/residue. A score above 0.2 showed that the F1 structure was correctly folded. In addition, the evaluation was performed using Errat, which analyzes the statistics of nonbonded interactions between atom types. A plot of the final model revealed approximately 96.3% of the sequence, which was below the 95% confidence level limit. For a fully refined structure, the sequence with a percentage that is below the 95% confidence level confirms that the structure is significantly correct.

The final structures of F1 protease and thermitase were superimposed to measure the accuracy of the corresponding target model to its template structure, which was demonstrated by Cα atoms that matched with a RMSD of 0.223 Å. Based on this value, the final model of F1 protease was obtained, with an accurate structure. The final structure of F1 protease exhibited 280 residues with 2,096 protein molecules. Similar to other serine proteases, we demonstrated that F1 protease contained a catalytic triad, comprising Asp 39, His 72, and Ser 226 (Fig. 2A). The predicted structure of F1 protease comprised 10 α-helices and 10 β-sheets that were arranged in a single domain. The schematic representation is shown in Fig. 2B.

Structural Comparison and Mutation Sites

Structural analysis and comparison were performed as described in Materials and Methods. Structural comparison and structure-based alignments between the crystal structures of three other subtilisin proteases (thermostable enzymes with different optimum temperatures) with F1 protease revealed a trend in the structures that might correlate with the increasing thermostability of these enzymes (Fig. 1). However, the results indicate the presence of interactions between ion pairs based on significant differences between the structures. The structural comparisons of serine proteases from subtilisin BPN', F1 protease, stetterlysin, and pyrolysin, which displayed the decreasing trend in thermostability of pyrolysin > stetterlysin > F1 protease > subtilisin BPN', revealed a tremendous increase in number of ion pairs in proteins. These results are consistent with the increased optimum temperature for each of the enzymes (Table 2). However, no highly conserved residues were detected in aromatic pairs, and each enzyme seemed to use a different set of aromatic residues for stabilization.

As shown in Fig. 3, structural comparison of F1 protease and stetterlysin revealed that the ion pair networks of F1 protease (Asp202, Arg250, Glu254) (Fig. 3A) and stetterlysin (Asp394, Lys458, Glu462) (Fig. 3B) were conserved with each other, with the exception of Trp200, which was replaced with Arg in stetterlysin. An ion pair network of F1 protease (Asp58, Asp61, Arg103) (Fig. 3C) was not

Table 2. Features of serine proteases that may be related to thermostability.

	Subtilisin BPN' [39,13]	F1 protease [9]	Stetterlysin [39]	Pyrolysin [39]
Optimal growth temperature host (°C)	30	70	75	100
Half-life values	23 min/60°C	4 h/85°C	2.5 h/100°C	4 h/100°C
Ion pairs	9	13	21	34
Disulfide bonds	0	1	0	0
Aromatic interactions	7	12	14	15

present in subtilisin BPN'. Therefore, to evaluate the effects of these ion pairs on protein stability, the mutants W200R (Trp at position 200 was replaced by Arg as in stetterlysin) and D58S (Asp at position 58 was replaced by Ser as in subtilisin BPN') were designed (Fig. 1). W200R and D58S mutations added a potential ion pair or disrupted an existing ion pair in F1 protease, respectively.

Arg; a positively charged residue was chosen instead of lysine to replace Trp at position 200, based on its properties. The properties of Arg residues suggest that these residues improve the enzyme's ability to adapt to high temperatures compared with lysine residues (also positively charged residue). First, the Arg δ-guanido moiety has a reduced chemical reactivity due to its high pKa and its resonance stabilization. The Arg δ-guanido moiety provides more surface area for charged interactions compared with the lysine amino group. Second, because the Arg side chain contains one fewer methylene group than lysine, the Arg

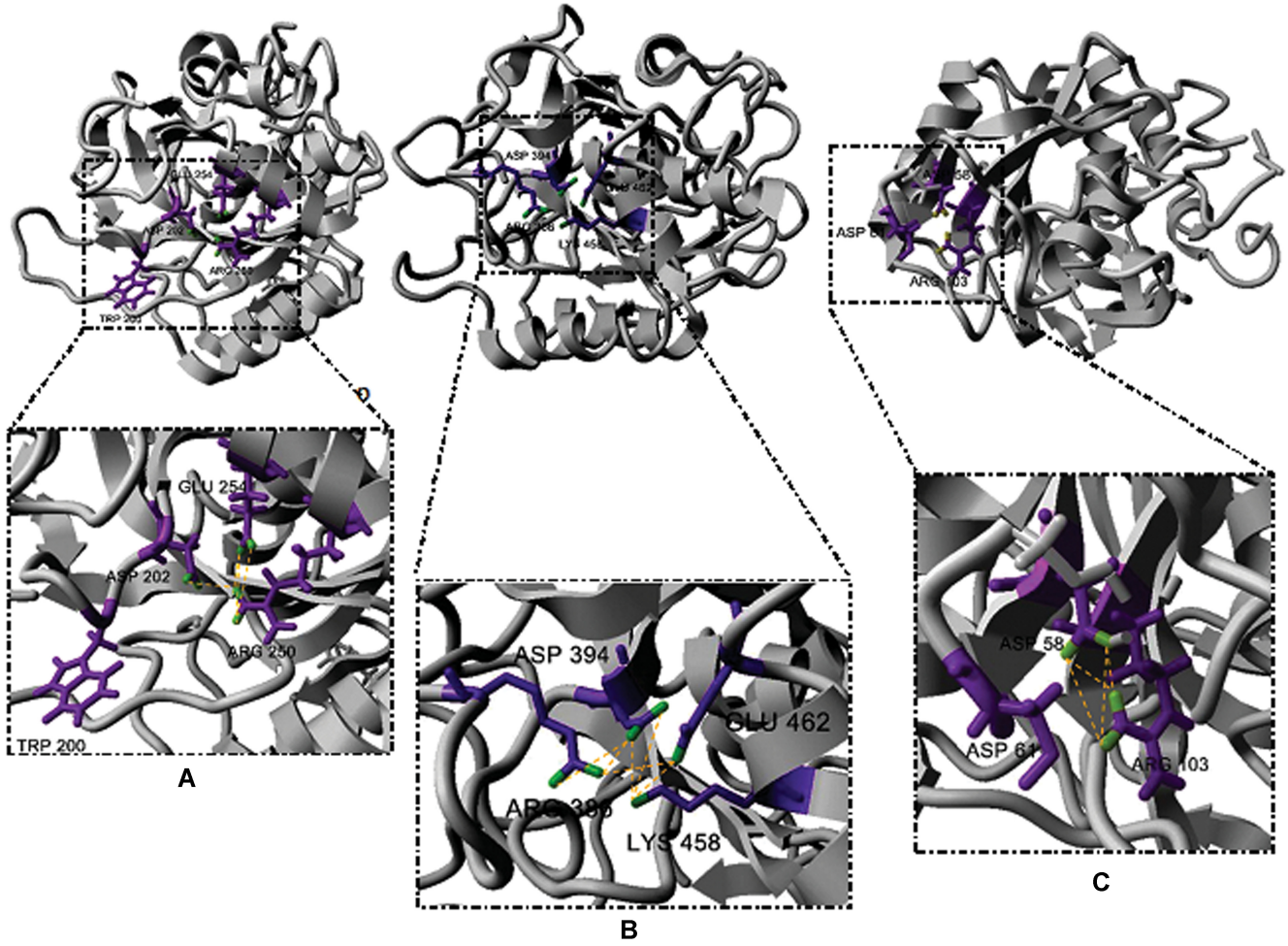

Fig. 3. Structural comparison of F1 protease and stetterlysin.
The models revealed that the ion pair network of F1 protease (Asp202, Arg250, Glu254) (**A**) and stetterlysin (Asp394, Lys458, Glu462) (**B**) could be conserved with each other, except for Trp200, which was replaced with Arg in stetterlysin. An ion pair network of F1 protease (Asp58, Asp61, Arg103) (**C**) was not present in subtilisin BPN'.

chain may develop fewer unfavorable contacts with the solvent [38]. Finally, because its pKa (approximately 12) is one unit above that of lysine (11.1), Arg can easily maintain ion pairs and has a net positive charge at elevated temperature (pKa value drops as the temperature increases) [23]. Substitution of Ser for Asp at position 58 (in the β-sheet) in F1 protease was located more than 10 Å away from the active site. Ser was chosen based on subtilisin BPN' (less stable than F1 protease). Ser at position 58 does not contribute to the ion pair networks in subtilisin BPN'. This substitution disrupted the existing ion pairs and destabilized the F1 protease structure.

Molecular Dynamics of mutated F1 Protease Structures

Molecular dynamics (MD) simulation techniques were used to analyze the dynamics behavior of two mutant proteases (W200R and D58S) and the recombinant F1 protease. Energy minimization was performed before the molecular dynamics simulations procedure to remove poor contacts and geometry [7].

In this study, RMSD was analyzed to characterize the conformational changes of the structure [21]. RMSD measures the evolution of conformational changes in the structure from the initial conformation [7, 25]. The RMSD for the W200R mutant reached a plateau early in the simulation, which was after 150 ps, and equilibrated at approximately 1.2 throughout the entire simulation period. The recombinant F1 protease and D58S mutant deviated further from the initial structure, rising steadily and reaching a plateau only after 300 ps. The RMSD equilibrated around 1.4 throughout the entire simulation period, with the exception of a small peak at 660 ps for the D58S mutant (Fig. 4). Comparative analysis of average structures at 360 K in water molecules suggested that the W200R mutant structure was more stable than those of the recombinant F1 protease and D58S mutant. However, the overall RMSD values for all proteases were considerably small, indicating that the structure after simulation was not significantly different from the initial structure and that the protease

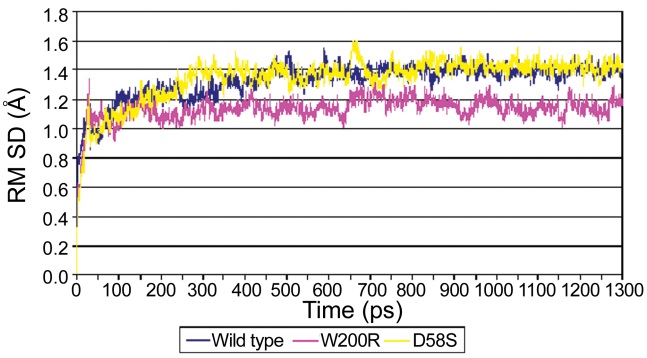

Fig. 4. Root mean squared deviation (RMSD) for the wild-type F1 protease, W200R mutant, and D58S mutant as a function time.

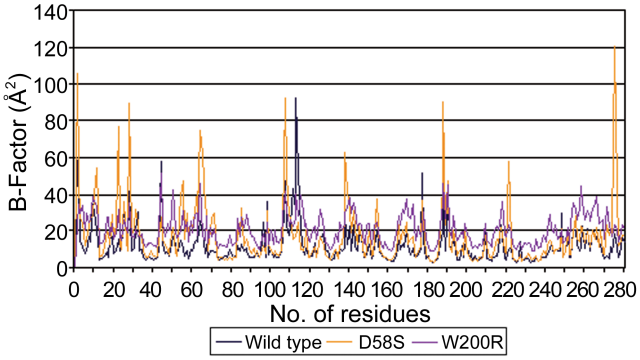

Fig. 5. B-factor for the wild-type F1 protease, W200R mutant, and D58S mutant structures.

structures were able to maintain their conformation [10]. The stable trajectories were obtained at approximately 1,000 ps and were used for the B-factor analysis.

Using the B-factor analysis, the D58S mutant structure showed more peaks (fluctuations) than the recombinant F1 protease structure. Therefore, we concluded that the recombinant F1 protease structure was more rigid than the D58S mutant structure. It is interesting to note that these flexibilities were not observed in the W200R mutant structure. The B-factor value for residues in the W200R mutant was dramatically decreased compared with nearly all of the residues that were highly flexible in the recombinant F1 protease and D58S mutant structures (Fig. 5). However, increased flexibility was observed in specific regions of the W200R mutant structure, which was indicated by a higher B-factor value compared with the recombinant F1 protease structure. However, no extremely high peaks were observed. Therefore, we concluded that the W200R mutant was rigid. It must be noted that proteins require some flexibility, which is vital for its function. Excessive rigidity explains why hyperthermophilic enzymes are inactive at low temperatures [38]. Therefore, it is not surprising that our results reveal few fluctuations (or low flexibility) in all protein regions.

The W200R mutant and D58S mutant were analyzed for possible ion pair formation in comparison with recombinant F1 protease. The distances of charged side chains near the mutation site were measured to assess ion pair formation. The distance was measured from the average structures of the recombinant F1 protease, and W200R and D58S mutants using the last 1,000 ps of the simulation period. Comparative analysis of the average structures revealed increased ion pair formation in the W200R mutant. In the recombinant F1 protease, the largest ion pair network was composed of three amino acid residues (Asp202, Arg250, Glu254) that were connected by four ion pairs (Fig. 6A). In contrast, the largest ion pair network consisted of four amino acid residues (Arg200, Asp202, Arg250, Glu254) that were connected by seven ion pairs in the W200R

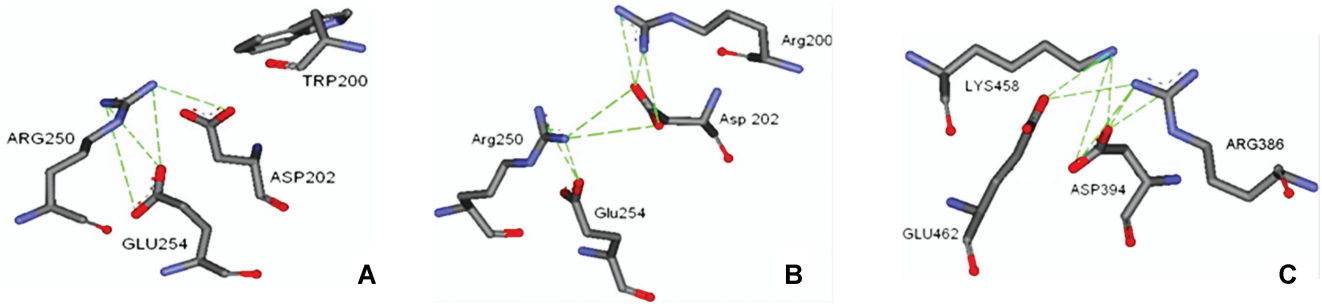

Fig. 6. Ion pairs network in wild-type F1 protease, W200R mutant, and stetterlysin structures.
(**A**) Wild-type of F1 protease structure; (**B**) W200R mutant structure; (**C**) stetterlysin structure showing the largest ion pairs network after molecular dynamics simulation.

mutant. The Arg200 contributed three new additional ion pairs with Asp202: NH1-OD1 (3.08 Å), NH1-OD2 (2.82 Å), and NH2-OD2 (3.20 Å) (Fig. 6B). The distance from these pairs was almost below 4.0 Å (between 2.82 and 3.20 Å) throughout the simulation (data not shown). This result indicates that ion pairs are maintained throughout the entire simulation time. In addition, this result shows that increasing numbers of ion pairs (similar to the hyperthermophilic stetterlysin, Fig. 6C) may increase the thermostability of F1 protease. Some of the ion pair interactions gave rise to hydrogen bond networks that linked different secondary elements and increased the unfolding resistance [25]. Bakker *et al.* [2] have performed MD simulations on Sac7d from the hyperthermophile *Sulfolobus acidocaldarius* at 300, 360, and 500 K. They have concluded that the ion pairs favorably contribute to protein stability at elevated temperatures. These findings confirm that ion pairs may significantly contribute to the thermal stability of the W200R mutant.

The recombinant F1 protease had other ion pair networks that were formed by Asp58, Asp61, and Arg103. The Asp58 and Arg103 were connected by four ion pairs and were linked at two β-sheets (Fig. 3C and 7A). The distances were approximately 2.85 Å and 3.41 Å. The mutation of D58S disrupted these four ion pairs and was replaced by a hydrogen bond between NH2-OG with a distance that was greater than 4 Å (Fig. 7B). This substitution affects structural instability. Furthermore, serine (Ser) is known as the best residue for interacting with water molecules that surround the protein structure [22]. In water, Ser interacts with a water molecule (usually mediated by a hydrogen bond), which is released at higher temperatures. This interaction may be changed to promote protein instability [24]. Therefore, thermophilic proteins have evolved to possess a low frequency of Ser [26].

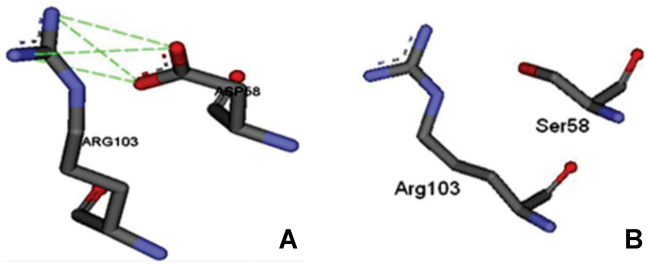

Fig. 7. Ion pairs network in wild-type F1 protease and D58S mutant structure.
Ion pairs network in (**A**) wild-type of F1 protease structure (**B**) D58S mutant structure.

Expressions of the Recombinant F1 Protease and Mutated Genes in *E. coli*

PCR primers were designed to introduce oligonucleotide-directed mutations into the F1 protease gene as described in Material and Methods. The mutations were confirmed using nucleotide sequencing. The results show the recombinant pGEX-4T1 vector provided high expression levels of recombinant F1 protease and both mutants compared with recombinant pTrcHis (data not shown). Therefore, *E. coli* BL21(DE3)pLysS harboring recombinant pGEX/recombinant F1 protease, pGEX/W200R mutant, and pGEX/D58S mutant genes were cultured in a liquid medium. The expressed proteases were purified using affinity chromatography and heat denaturation.

Effects of Mutation Sites

The effects of substitutions on the stability of F1 protease were studied using RMSD, β-factor analysis, and ion pair interactions through molecular dimension simulations. The results have been discussed above. To integrate the computational and experimental data, the thermostability test and CD structure analysis were performed. Fig. 8 shows that the recombinant W200R mutant had half-lives of 75 min and 12 min at 85°C and 90°C, respectively. Meanwhile, the recombinant wild-type F1 protease had half-lives of 60 min and 7 min at 85°C and 90°C, respectively. However, the recombinant D58S mutant had a half-life of 45 min at 85°C. No protease activity was detected when

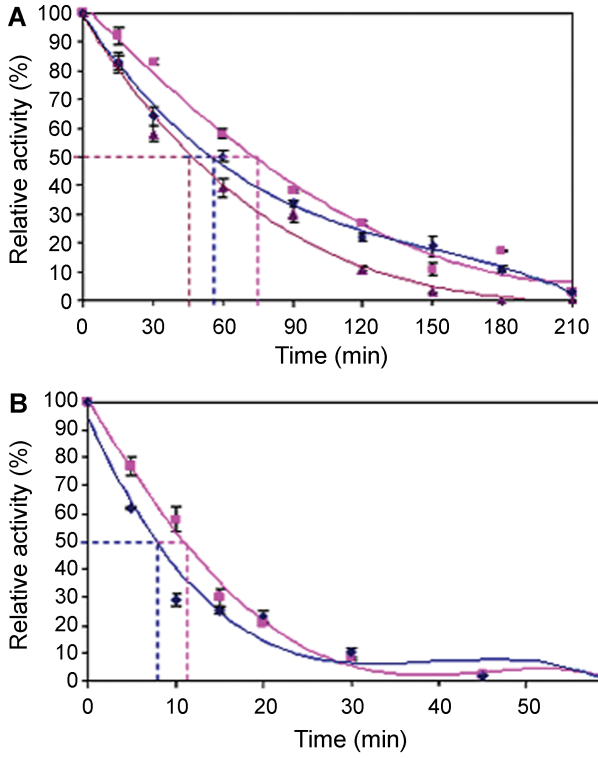

Fig. 8. Effect of different temperatures on enzymes stability.
The enzymes (◆) wild-type F1 protease, (■) W200R mutant, and (▲) D58S mutant in Tris-HCl–2 mM Ca^{2+} (pH 9.0) were pre-incubated for various times at 85°C (**A**) and 90°C (**B**). Error bars represent standard deviations of triplicate determinations. Note: There was no protease activity detected for D58S when this protein was incubated at 90°C.

this protein was incubated at 90°C. The data showed that the half-lives of the recombinant W200R mutant were 1.25 to 1.7 times longer and considerably more stable than the recombinant F1 protease. The recombinant D58S mutant was less stable than the recombinant F1 protease.

Far-UV CD measurements allowed us to evaluate the overall features of the secondary structure of the protein and to quantify the relative proportions of α-helices, β-sheets, and random coils [8]. The CD spectra of both mutants exhibited similar profiles to that of the recombinant F1 protease. Fig. 9 shows that the recombinant F1 protease, W200R mutant, and D58S mutant exhibited two negative peaks centered at approximately 209 and 221 nm. The appearance of these peaks is suggestive of significant α-helical content. A positive peak from approximately 195–200 nm was detected in all proteins. This peak suggested that these proteins have β-sheet content. β-Sheet content was detected in the recombinant F1 protease, W200R mutant, and D58S mutant at approximately 210–220 nm (negative spectrum). The best spectrum for β-sheet content was at approximately 210–215 nm. The best spectrum for α-helix content was at approximately 207 and 220 nm, as previously reported [14]. The secondary

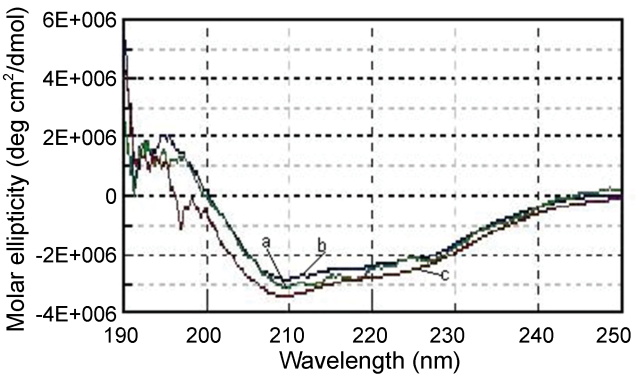

Fig. 9. Secondary structure of wild-type F1 protease and variants.
(a) The far UV CD spectra of the wild-type F1 protease, (b) the W200R mutant, and (c) the D58S mutant.

structure studies of the recombinant F1 protease, W200R mutant, and D58S mutant are summarized in Table 3. We detected an increase of 3.8% and 1.7% of α-helices and random coils, respectively, in the W200R mutant. However, a small decrease in α-helices and an increment up to more than 8% of random coils were observed in the D58S mutant. In contrast, there was some loss of β-sheets in the W200R and D58S mutants compared with the recombinant wild-type F1 protease.

This result indicates that the addition or disruption of ion pairs with a single residue replacement may affect the secondary structure of a protein. A single replacement of Trp200 with Arg as in W200R protease stabilizes the α-helix. Arg200 was located in a turn region that extensively interacted with an α-helix. Disruption of four ion pairs between Asp58 and Arg103, which was observed in the D58S mutant, was located in the β-sheet and caused minor structural changes, such as loosening of the secondary structure and the loss of the β-sheet. Similarly, Rahman *et al*. [31] have reported that all recombinant enzymes (P*k*-GDH, P*k*-GDH-T138E, P*k*-GDH-E158Q) possess different structures from that of natural GDH. In another report, it has been demonstrated that the replacement of Ala47 with the bulky side chain of Phe in propeptide subtilisin BPN' contributes to the structural changes that accompany an

Table 3. Protein secondary structure analysis of the wild-type F1 protease, W200R mutant, and D58S mutant at 20°C.

Secondary structure	Ratio (%) at 20°C		
	Wild type	W200R mutant	D58S mutant
α-Helix	25.5	29.3	24.0
β-Sheet	17.7	14.5	14.1
Turn	22.5	20.5	20.0
Random	34.0	35.7	41.9

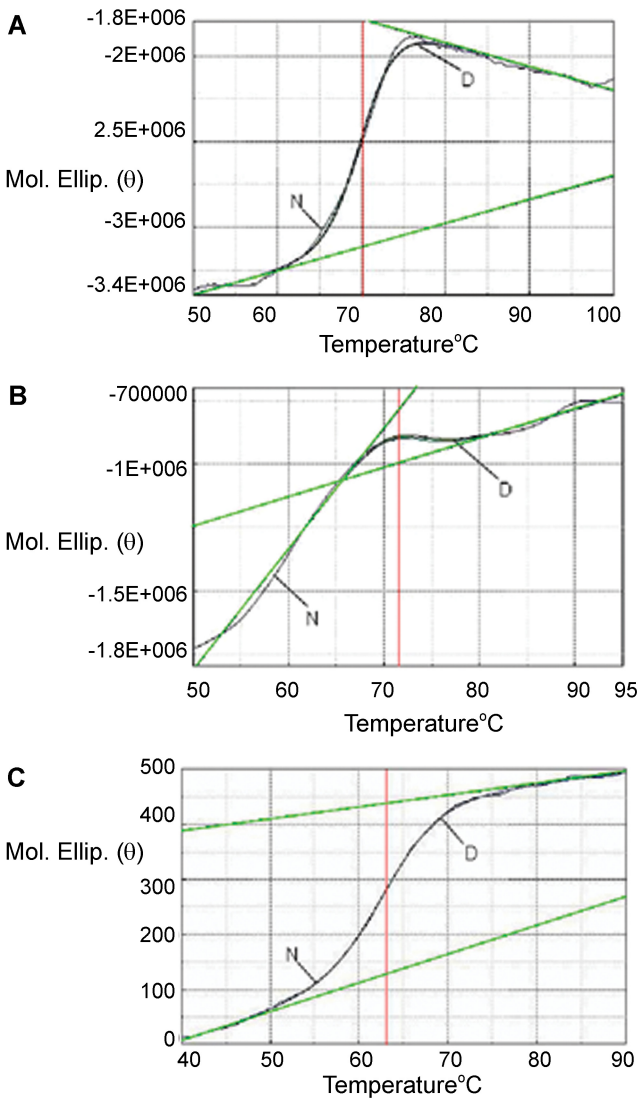

Fig. 10. Denatured protein analysis of the (**A**) F1 protease, (**B**) W200R mutant, and (**C**) D58S mutant.
The melting points (—) of unfolding protein at 221 nm for F1 protease, W200R mutant, and D58S mutant are 70°C, 72°C, and 63°C, respectively. The fitting lines (—) corresponding to the native (N) and denatured (D) states of the D58S mutant are shown on the melting curves.

increase in the secondary structure, which increases its hydrophobicity [16].

The thermal denaturation study was performed using the far-UV CD spectrum. In this study, far-UV CD at 221 nm was used to detect the denatured protein of recombinant F1 protease and both mutants owing to the far-UV CD spectra of secondary structures. As the temperature was increased from 50°C to 90°C, the change in ellipticity at 221 nm revealed a sigmoidal monophasic transition curve for all proteins, indicating protein unfolding (Fig. 10). The melting points (T_m values) at pH 8.0 of recombinant F1 protease (Fig. 10A), the W200R mutant (Fig. 10B), and the D58S mutant (Fig. 10C) were 70°C, 72°C, and 63°C, respectively.

Integration of Computational and Experimental Data

Based on the secondary structure of W200R, the results indicate that Arg200 may stabilize the α-helix content. In the computational study, Arg200, which is located at a turn region, extensively interacted with an α-helix. This interaction involves the largest ion pair network (seven ion pairs) in the W200R mutant. The increase of α-helix in the W200R mutant may be related to the additional ion pairs in this mutant. MD simulations confirmed a reduced mobility or flexibility in the W200R structure due to additional ion pairs. Therefore, the W200R mutant was more rigid compared with the wild-type protein. Decreased flexibility and increased hydrophobicity are common characteristics of more thermostable proteins. Flexibility (and also hydrophilicity) that is decreased at α-helical segments, which are located at non-buried or surface positions in helices, may be predominant in thermo-adaptation. Helices are the most stable and fast-folding structural units and may be ideal candidates to increase thermostability [1]. The heat stability, which was determined by the trend of the melting curve (T_m), showed that the W200R mutant was stable, with a T_m of 72°C. In addition, the thermostability test revealed that the W200R mutant had a longer half-life compared with the recombinant wild-type F1 protease. This result indicates that an additional ion pair in the W200R mutant is effective in increasing its thermostability.

In contrast, the D58S mutant was less resistant to denaturation and to temperature changes, with a shift in T_m of 7°C compared with that of the recombinant protein. In addition, the D58S mutant exhibited a decreased half-life compared with that of the recombinant wild-type F1 protease. It is important to point out that substitution of Asp58 with Ser disrupted four ion pairs between Asp58 and Arg103, which were located in the β-sheet. As a result, the mutation may alter the conformation of the region around this residue, leading to a change in the pattern of β-sheet content. Therefore, the D58S mutant was less stable, which may be due to the removal of four intermolecular ion pairs in a protein, as suggested in the simulation studies. A dramatic change was observed in the D58S structure, which was more flexible than that of the recombinant F1 protease. These results indicate that intermolecular ion pairs influence the enzyme thermostability of F1 protease.

Acknowledgment

This work was supported by a Science Fund Research Grant from MOSTI (Ministry of Science, Technology and Innovation), Malaysia.

References

1. Arias, L. M. and P. Argos. 1989. Engineering protein thermal stability; sequence statistics point to residue substitutions in α-helices. *J. Mol. Biol*. **206:** 397–406.
2. Bakker, P. I. W., P. H. Hunenberger, and J. A. McCammon. 1999. Molecular dynamics simulations of the hyperthermophilic *Sulfolobus acidocaldarius*: Contribution of salt bridges to thermostability. *J. Mol. Biol*. **285:** 1811–1830.
3. Braxton, S. B. and J. A. Wells. 1991. Incorporation of a Ca-binding loop into subtilisin BPN'. *Biochemistry* **31:** 7796–7801.
4. Bryan, P. N. 2000. Protein engineering of subtilisin. *Biochim. Biophys. Acta* **1543:** 203–222.
5. Choi, I. G., W. G. Barg, S. H. Kim, and Y. G. Yu. 1999. Extremely thermostable serine-type protease from the *Aquifex pyrophilus. J. Biol. Chem.* **274:** 881–888.
6. Colovos, C. and T. O. Yeates. 1992. Verification of protein structures: Patterns of non-bonded atomic interaction. *Protein Sci*. **2:** 1511–1519.
7. El-Bastawissy, E., M. H. Knaggs, and I. H. Gilbert. 2001. Molecular dynamics simulations of the wild-type and point mutation human prion protein at normal and elevated temperature. *J. Mol. Graph Model* **20:** 145–154.
8. Fontana, A., P. P. de Laureto, B. Spolaore, E. Frare, P. Picotti, and M. Zambomin. 2004. Probing protein structure by limited proteolysis. *Acta Biochim. Pol*. **51:** 299–321.
9. Fu, Z., S. A. Hamid, C. N. A. Razak, M. BAsri, A. B. Salleh, and R. N. Z. A. Rahman. 2003. Secretory expression in *Escherichia coli* and single step purification of a heat-stable alkaline protease. *Protein Express. Purif*. **28:** 63–68.
10. Gsponer, J., P. Ferrara, and A. Caflisch. 2001. Flexibility of the murine prion protein and its Asp178Asn mutant investigated by molecular dynamics simulations. *J. Mol. Graph Model* **20:** 169–182.
11. Haki, G. D. and S. T. Rakshit. 2003. Developments in industrially important thermostable enzymes: A review. *Bioresour. Technol*. **89:** 17–34.
12. Jang, J. S., K. H. Bae, and S. M. Byun. 1992. Effect of the weak Ca^{2+} binding site of subtilisin J by site-directed mutagenesis on heat stability. *Biochem. Biophys. Res. Commun*. **188:** 184–189.
13. Karasaki, Y. and M. Ohno. 1979. Interactions of BPN' and Carlsberg subtilisin with peptides containing aromatic amino acids at the C-terminus: Specific rate enhancement due to the secondary enzyme–substrate interaction. *J. Biochem*. **86:** 563–567.
14. Katamari, Y. O., C. M. Dobson, and T. Konno. 2003. Structural dissection of alkaline-denatured pepsin. *Prot. Sci*. **12:** 717–724.
15. Knapp, S., W. M. de Vos, D. Rice, and R. Ladenstein. 1997. Crystal structure of glutamate dehydrogenase from the hyperthermophilic eubacterium *Thermotoga maritima* at 3.0 Å resolution. *J. Mol. Biol*. **267:** 916–932.
16. Kojima, S., T. Minagawa, and K. Miura. 1998. Tertiary structure formation in the propetide of subtilisin BPN' by successive amino acid replacements and its close relation to function. *J. Mol. Biol*. **277:** 1007–1013.
17. Kumar, S., C. Tsai, and R. Nussinov. 2000. Factors enhancing protein stability. *Protein Eng*. **13:** 179–191.
18. Laskowski, R. A., M. W. MacArthur, D. K. Smith, D. T. Jones, E. G. Hutchinson, A. L. Morris, *et al*. 1994. Procheck V.3.5.4: Operating Manual. http://www.biochemical.ucl.ac.uk/-roman/procheck/procheck.html.
19. Laemmli, U. K. 1970. Cleavage of structural protein during assembly of the head of bacteriophage T4. *Nature* **227:** 680–685.
20. Lüthy, R., J. U. Bowie, and D. Eisenberg. 1992. Assessment of the protein models with three-dimensional profiles. *Nature* **356:** 83–85.
21. Marti-Renom, M. A., J. M. Mas, B. Oliva, E. Querol, and F. X. Aviles. 1998. Effects of counter-ions and volume on the simulated dynamics of solvated proteins. Application on the activation domain of procarboxypeptidase B. *Protein Eng*. **11:** 881–890.
22. Mattos, C. 2002. Protein-interactions in a dynamic world. *Trends Biochem. Sci*. **27:** 203–208.
23. Mrabet, N. T., A. Van den Broeck, I. Van den Brande, P. Stanssens, Y. Laroche, A. M. Lambeir, *et al*. 1992. Arginine residues as stabilizing elements in proteins. *Biochemistry* **31:** 2239–2253.
24. Nagendra, H. G., N. Sukumar, and M. Vijayan. 1998. Role of water in plasticity, stability, and action of proteins: The crystal structures of lysozyme at very low levels of hydration. *Proteins* **32:** 229–240.
25. Okimoto, N., K. Yamanaka, A. Suenaga, Y. Hirano, N. Futatsugi, T. Narumi, *et al*. 2003. Molecular dynamics simulations of prion proteins: Effect of Ala^{117} to Val mutation. *Construction*. **3:** 1–11.
26. Pack, S. P. and Y. J. Yoo. 2004. Protein thermostability: Structure-based difference of amino acid between thermophilic and mesophilic proteins. *J. Biotechnol*. **111:** 269–277.
27. Padone, E., R. Cannio, M. Saviano, M. Rossi, and S. Bartolucci. 1999. Prediction and experimenal testing of *Bacillus acidocaldarius* thioredoxin stability. *Biochem. J*. **339:** 309–317.
28. Pantoliano, M. W., R. C. Ladner, P. N. Bryan, M. L. Rolence, J. F. Wood, and T. L. Poulos. 1987. Protein engineering of subtilisin BPN': Stabilization through the introduction of two cysteines to form a disulfide bond. *Biochemistry* **26:** 2077–2082.
29. Pantoliano, M. W., M. Whitlow, J. F. Wood, S. W. Dodd, K. D. Hardman, M. L. Rolence, and P. N. Bryan. 1989. Large increases in general stability for the subtilisin BPN' through incremental changes in the free energy of unfolding. *Biochemistry* **28:** 7205–7213.
30. Rahman, R. N. Z. A., C. N. Razak, K. Ampon, M. Basri, W. M. Z. W. Yunus, and A. B. Salleh. 1994. Purification and characterization of a heat-stable alkaline protease from *Bacillus stearothemophilus* F1. *Appl. Microbiol. Biotechnol*. **40:** 822–827.
31. Rahman, R. N. Z. A., S. Fujiwara, H. Nakamura, M. Takagi, and T. Imanaka. 1998. Ion pairs involved in maintaining a thermostable structure of glutamate dehydrogenase from a hyperthermophilic archeon. *Biochem. Biophys. Res. Commun*. **248:** 920–926.
32. Sali, A. and T. L. Blundell. 1993. Comparative modeling by satisfaction of the spatial restraints. *J. Mol. Biol*. **234:** 779–815.
33. Smith, C. A., H. S. Toogood, H. M. Baker, R. M. Daniel, and E. N. Baker. 1999. Calcium-mediated thermostability in the

subtilisin superfamily: The crystal structure of *Bacillus* Ak.1 protease at 1.8 Å resolution. *J. Mol. Biol*. **294:** 1027–1040.

34. Sorensen, S. B., L. M. Bech, M. Meldal, and K. Breddam. 1993. Mutational replacements of the amino acid residues forming hydrophobic S4 binding pocket of subtilisin 309 from *Bacillus lentus*. *Biochemistry* **32:** 8994–8999.
35. Takagi, H., T. Takahashi, H. Momose, M. Inouye, Y. Maeda, and H. Matsuzawa. 1990. Enhancement of the thermostability of subtilisin E by introduction of a disulfide bond engineered on the basis of structural comparison with thermophilic serine protease. *J. Biol. Chem*. **256:** 6874–6878.
36. Teplyakov, A. V., I. P. Kuranova, E. H. Harutyunyan, B. K. Vainshtein, C. Frömmel, W. E. Höhne, and F. S. Wilson. 1990. Crystal structure of thermitase at 1.4 Å resolution. *J. Mol. Biol*. **214:** 261–279.
37. Topf, M., M. L. Baker, M. A. Marti-Renom, W. Chiu, and A. Sali. 2006. Refinement of protein structures by iterative comperative modeling and cryoEM density fitting. *J. Mol. Biol*. **357:** 1655–1668.
38. Vieille, C. and G. J. Zeikus. 2001. Hyperthermophilic enzymes: Sources, uses and molecular mechanisms for thermostability. *Microbiol*. *Mol. Biol. Rev.* **65:** 1–43.
39. Voorhorst, W. G. B., A. Warner, W. M. de Vos, and R. J. Siezen. 1997. Homology modeling of two subtilisin-like serine proteases from the hyperthemophilic archaea *Pyrococcus furiosus* and *Thermococcus stetteri. Protein Eng*. **10:** 905–914.